Atmos. Meas. Tech. Discuss., doi:10.5194/amt-2016-17, 2016
Manuscript under review for journal Atmos. Meas. Tech.
Published: 25 January 2016

Atmospheric Measurement Techniques Discussions

HONO Measurement by Differential Photolysis

C. Reed[1], C. A. Brumby[3], L. R. Crilley[4], L. J. Kramer[4], W. J. Bloss[4], P. W. Seakins[2,3], J. D. Lee[1,2], L. J. Carpenter[1]

[1] Wolfson Atmospheric Chemistry Laboratories, Department of Chemistry, University of York, Heslington, York, YO10 5DD, United Kingdom

[2] NCAS, School of Earth and Environment, University of Leeds, Leeds, LS2 9JT, United Kingdom

[3] School of Chemistry, University of Leeds, Leeds, LS2 9JT, United Kingdom

[4] School of Geography, Earth and Environmental Sciences, University of Birmingham, B15 2TT, United Kingdom.

Correspondence to: James.Lee@york.ac.uk

Abstract

Nitrous acid (HONO) has been quantitatively measured *in-situ* by differential photolysis at 385 and 395 nm and subsequent detection as nitric oxide (NO) by the chemiluminescence reaction with ozone (O_3). The technique has been evaluated by FT-IR to provide a direct HONO measurement in a simulation chamber, and compared side-by-side with a LOng Absorption Path Optical Photometer (LOPAP) in the field. The NO/O_3 chemiluminescence technique is robust, well characterized and capable of sampling at low pressure whilst solid-state converter technology allows for unattended *in-situ* HONO measurements in combination with fast time resolution and response.

1 Introduction

Nitrous acid (HONO) is a major source of hydroxyl (OH) radicals in the boundary layer (Elshorbany et al., 2008; Kim et al., 2014; Levy II, 1973). HONO can be formed homogeneously through reaction of nitric oxide (NO) with OH, heterogeneously through several pathways, or emitted directly (Kleffmann, 2007; Lammel and Cape, 1996; Spataro and Ianniello, 2014; Su et al., 2011). HONO is formed heterogeneously on surfaces through the reaction of NO_2 with H_2O (Bröske et al., 2003). This heterogeneous formation of HONO is a net source of OH radicals in

Atmos. Meas. Tech. Discuss., doi:10.5194/amt-2016-17, 2016
Manuscript under review for journal Atmos. Meas. Tech.
Published: 25 January 2016

the troposphere and is an important mediator of air quality, particularly in polluted environments (Finlayson-Pitts et al., 2003; Gutzwiller et al., 2002; Lee et al., 2015). Direct emission of HONO through vehicle exhaust is also thought to be a source (Kirchstetter et al., 1996; Kurtenbach et al., 2001). Emission from snowpack has also been documented (Beine et al., 2008; Zhou et al., 2001) and more recently biogenic sources of HONO have been identified from nitrite producing bacteria (Oswald et al., 2013; Su et al., 2011), and soil crusts (Weber et al., 2015).

In urban areas HONO can be the major net source of OH (discounting radical cycling driven by e.g. NO), contributing up to 80% of daytime OH production in winter and 50% in summer (Elshorbany et al., 2008; Kleffmann, 2007; Villena et al., 2011b). However, the sources of HONO and the many processes by which it forms are not well understood (Kleffmann et al., 2006; Sörgel et al., 2011; Spataro and Ianniello, 2014; Villena et al., 2011a). There is a clear need for *in-situ* measurement of HONO in order to better understand its chemistry and emissions.

Currently, methods of detecting HONO are either remotely through DOAS (Febo et al., 1996; Hendrick et al., 2014; Stutz et al., 2010), or by filter/denuder sampling (Acker et al., 2005, 2006; Febo et al., 1993, 1996; Ianniello et al., 2007). A variety of *in-situ* techniques exist, namely: Quantum Cascade-Tuneable Infrared Laser Differential Absorption Spectrometer (QC-TILDAS) (Lee et al., 2011); Ion Drift Chemical Ionization Mass Spectrometer (ID-CIMS) (Levy et al., 2014); Ambient Ion Monitor - Ion Chromatography (AIM-IC) (Markovic et al., 2012; Vandenboer et al., 2014); Stripping-Coil Visible Absorption Photometry (SC-AP) (Ren et al., 2011); Negative-Ion Proton-Transfer Chemical Ionization Mass Spectrometry (NI-PT-CIMS) (Roberts et al., 2010); Incoherent Broadband Cavity Enhanced Absorption Spectroscopy (IBBCEAS) (Pusede et al., 2014); dedicated commercial on-line, *in-situ* measurements include Dual Laser – Quantum Cascade Laser (Aerodyne Research) and, as used in this study, Long Path Absorption Photometer (LOPAP) (Heland et al., 2001). LOPAP has been characterized quite extensively by other authors e.g. (Clemitshaw, 2004; Kleffmann and Wiesen, 2008; Kleffmann et al., 2006, 2013; Ródenas et al., 2013).

Atmos. Meas. Tech. Discuss., doi:10.5194/amt-2016-17, 2016
Manuscript under review for journal Atmos. Meas. Tech.
Published: 25 January 2016

Atmospheric Measurement Techniques Discussions

Here, we demonstrate the exploitation of a known HONO interference for photolytic NO_2 conversion systems (Pollack et al., 2011; Ryerson et al., 2000; Sadanaga et al., 2010, 2014; Villena et al., 2012), to provide a simple photolytic technique for quantitative analysis of HONO.

2 Experimental

The differential photolytic HONO technique, henceforth referred to as pHONO, was developed from an existing fast NO_x analyser described in section 2.1. The photolytic converter is described specifically in section 2.2. Calibration is described in 2.3.

2.1 Differential Photolysis instrument

Measurement were performed using a dual channel Air Quality Design Inc. (Golden, Colorado, USA) instrument equipped with a UV-LED based photolytic NO_2 converter – commonly referred to as a Blue Light Converter (BLC) as described in Reed et al. (2015).

Briefly, two NO chemiluminescence analysers operate in parallel with duplicated independent equipment. The analysers share a common inlet allowing for parallel calibration of each channel. One channel is equipped with a photolytic NO_2 converter so that NO_x can be determined with that channel whilst also measuring NO concurrently. This allows for fast (1 Hz or greater) determination of NO and NO_2.

In order to be able to also measure HONO, the NO_x channel was redesigned so that the photolytic converter (section 2.2) operates in a switching mode. That is, the two lamps of different wavelengths operate alternately on a 50% duty cycle. Practically, the lamps switch every 30 seconds allowing for ca. 1 minute time resolution data.

2.2 NO_2/HONO photolytic converter

Photolytic converters were based on those supplied by Air Quality Design and manufactured according to their proprietary standards (Buhr, 2004, 2007) and are described in Reed et al., (2015). Practically, two UV-LED arrays are positioned at opposing ends of a cavity which is highly reflective to UV. Sample gas is introduced at one end of the illuminated cavity, exiting at the other. NO in the sample exiting the converter is enhanced over the original by photolysis of NO_2 or HONO, thus by calibration of the conversion efficiency these can be quantified.

Atmos. Meas. Tech. Discuss., doi:10.5194/amt-2016-17, 2016
Manuscript under review for journal Atmos. Meas. Tech.
Published: 25 January 2016

Atmospheric Measurement Techniques Discussions

Modifications were made to the control of the UV-LED elements to allow independent switching of the lamps. The wavelength of one lamp was changed from standard (395 nm) to 385 nm in order to overlap better with the HONO absorption spectrum, while the actual UV-LEDs (3 watt, LED Engin, Inc.) are more efficient and higher powered than those used in previous work (Reed et al., 2015).

The volume of the illuminated sample chamber is 16 mL which, with a standard flow rate of 1 standard L per min^{-1} gives a sample residence time of 0.96 seconds at standard atmospheric temperature and pressure (SATP). The $NO_2 \rightarrow NO$ conversion efficiency of the standard BLC with the sample flow of 1 standard L per min^{-1} was ~89 % with both lamps illuminated. Individual lamp conversion efficiencies were 72.9 and 81.3 % ±0.1 for the 385 and 395 nm lamps respectively. Determination of the conversion efficiency is detailed in section 2.4.

2.3 Characterisation

Spectral radiograms of the UV-LEDs output were obtained using the same procedure and equipment described in Reed et al., (2015) using an Ocean Optics QE65000 spectral radiometer coupled to a 2π quartz collector within a light sealed chamber.

Figure 1 shows the measured spectral emission of two UV-LED units of two different wavelengths; 385 and 395 nm. Also shown is the absorption cross-section of HONO, $BrONO_2$, and the NO_2 quantum yield (Sander et al., 2006). It is clear that there is greater overlap, calculated to be 30%, of the HONO absorption features with the 385 nm LED than at 395 nm. In R2 we see that NO is produced stoichiometrically through the photolysis of HONO. In this way, illuminating an air sample at either wavelength yields a signal, we shall denote as $NO_2^{\dagger}$; which represents the sum of contributions from NO_2 and HONO (R1 + R2) in differing proportions depending upon wavelength.

$$NO_2 + h\nu(<410nm) \rightarrow NO + O(^3P) \quad \text{(R1)}$$

$$HONO + h\nu(<390\ nm) \rightarrow NO + OH \quad \text{(R2)}$$

The difference in $NO_2^{\dagger}$signal measured at 385 and 395 nm corresponds to the difference in conversion efficiency of HONO and NO_2 between the two wavelengths. Differences in NO_2

Atmos. Meas. Tech. Discuss., doi:10.5194/amt-2016-17, 2016
Manuscript under review for journal Atmos. Meas. Tech.
Published: 25 January 2016

conversion efficiency of each lamp may be readily calibrated for and so taken into account (see section 2.4). The difference in $NO_2^{\dagger}$signal measured at 385 and 395 nm can therefore be used to calculate the HONO present in the sample Eq. (1);

$$\frac{NO_2{}^{\dagger}{}_{385} - NO_2{}^{\dagger}{}_{395}}{HONO\ CE_{385} - HONO\ CE_{395}} = [HONO] \qquad (1)$$

Apparent HONO conversion efficiency (CE), HONO CE_{385} – HONO CE_{395}, is determined experimentally as described in section 2.4.

It is noted that at both 385 nm and 395 nm there is potential interference from $BrONO_2$ (or in fact any other compounds which photolyse to give NO at either wavelength), with similar spectral overlap (Figure 1). Assuming a quantum yield of 1 integrated over all wavelengths for $BrONO_2$, 21.5 ppt of $BrONO_2$ at 385 nm and 18.1 ppt at 395 nm would be required to produce a 1 ppt error in the NO_2/HONO signal. Due to the low abundance (< 10 pptV) of $BrONO_2$ in the lower atmosphere (Yang et al., 2005), interference is therefore likely to be minimal (Pollack et al., 2011). The difference in conversion for the different lamps equates to a maximum error in HONO determination of 3.4 % [$BrONO_2$]; typically much less than 1 ppt.

The NO + OH back reaction after an air sample has exited the photolytic converter, but before entering the high vacuum of the analyser, causing a decrease in signal from HONO is discussed in Sec. 2.4.

2.4 HONO and NO_2 Conversion Efficiencies

The NO_2 – HONO converter system was calibrated for both NO_2 and HONO conversion efficiency. NO_2 conversion efficiencies were determined following the procedure outlined by Lee et al., (2009). The sensitivity of a detector in counts per second per part per trillion (cps/ppt) is determined by adding a 7.5 mL min^{-1} mass flow controlled flow (MFC) of NO calibration gas (4.78 ppm NO in N_2, BOC) to the inlet of the analyser whilst sampling an overflow of zero air free from NO_x, VOC and ozone. This equates to a calibration concentration of 12.5 ppbV NO per channel. Zero air was generated by scrubbing dried (-40 T_d) compressed air using Sofnofil (Molecular Products) and activated charcoal (Sigma Aldrich) traps. As described by Reed et al., (2015) this combination results in the lowest NO_2 signal. The sensitivity was found to be ~ 6.8

Atmos. Meas. Tech. Discuss., doi:10.5194/amt-2016-17, 2016
Manuscript under review for journal Atmos. Meas. Tech.
Published: 25 January 2016

and ~ 6.4 (±5%) cps/ppt for the NO and NO_x channels, respectively. In order to determine the NO_2 converter efficiency a portion of the NO added to the inlet is first titrated to NO_2 by reaction with ozone, typically generating 10.0 ppbV NO_2. Ozone is generated by illuminated a small flow (~10 mL min^{-1}) of O_2 with a broad output low pressure mercury UV lamp (BHK Inc.) The analyser signal (photomultiplier counts in Hz) is then recorded with neither UV-LED illuminated, and then with each illuminated in turn to determine the increase in signal arising for each lamp. The conversion efficiency (CE) is then determined as in Eq. (2).

$$CE = 1 - \frac{Signal_{Untitrated} - Signal_{Illuminated}}{Signal_{Untitrated} - Signal_{Titrated}} \quad (2)$$

The NO_2 conversion efficiency was determined to be 72.9 (j = 1.3 s^{-1}) and 81.2 % (j = 1.7 s^{-1}) ±0.1 for the 385 and 395 nm lamps, respectively.

Calibration for HONO was achieved by sampling a permeation source over a range of dilutions using methods modified from Taira and Kanda, (1990) and Febo et al., (1995). Nitrous acid was generated by the reaction of hydrochloric acid with sodium nitrite salt as described by Febo et al., (1995) shown in reaction 3.

$$HCl + NaNO_2 \rightarrow HONO + NaCl \quad (R3)$$

In order to achieve a continuous source of HONO, a permeation tube (Kin-Tek, HRT-010.00-BLANK/U) was filled with HCl (37%, Fluka, AR grade) and placed in a thermostated (30 to 55 ^{o}C) permeation oven (Kin-Tek, 585) with $NaNO_2$ salt (Fluka, AR grade). The permeation oven was flushed with 1.5 standard L min^{-1} zero air. The reaction is limited by HCl which permeates at a low rate thus allowing low concentrations (<50 ppb) of HONO to be generated continuously.

As side products of reaction 3 can also be produced, the output of the permeation source was continuously analysed for impurities. In reaction 4 NO and NO_2 can be formed by the gas phase self-reaction of HONO. In reaction 5, HNO_3 can be formed by reaction between adsorbed and gas phase HONO.

$$2HONO_{(g)} \rightarrow NO + NO_2 + H_2O \quad (R4)$$

$$HONO_{(ads)} + NO_2 \rightarrow HNO_3 + NO \quad (R5)$$

Atmos. Meas. Tech. Discuss., doi:10.5194/amt-2016-17, 2016
Manuscript under review for journal Atmos. Meas. Tech.
Published: 25 January 2016

To quantify HONO without any direct measurement and close the nitrogen balance, NO, NO_2, and total NO_y (NO + NO_2 + other reactive oxidised nitrogen species such as HNO_3, HONO, PAN) were measured continuously. The differential photolysis instrument itself was used to quantify the NO. NO_2 was measured directly by Cavity Attenuated Phase Shift (CAPS) spectroscopy (Kebabian et al., 2005, 2008) using an EPA certified Teledyne API T500U, to avoid any HONO interference (which would have been present in a photolytic measurement). Total NO_y was quantified using a Thermo Environmental 42c TL NO_x analyser equipped with a molybdenum catalytic converter which has been shown to quantify NO_y species such as HONO and HNO_3 (Clemitshaw, 2004; Fehsenfeld et al., 1987; Villena et al., 2012; Williams et al., 1998). The TEI 42c TL and Teledyne API T500U were calibrated either directly with an NO standard or by gas phase titration of NO to NO_2 using a Monitor Europe S6100 Multi Gas Calibrator. Production of HNO_3 (R5) would be indicated by an enhancement in NO over NO_2, as NO and NO_2 are produced stoichiometrically through the self-reaction of HONO (R4), whereas HNO_3 production consumes NO_2 and produces NO. Thus, HNO_3 can be indirectly quantified by the NO: NO_2 ratio, and was found to be a minimal contribution to total NO_y. As such, HONO can reasonably be presumed to be equivalent to $[NO_y] - ([NO] + [NO_2] + [HNO_3])$. Measured quantities are shown in table 1.

The stability of the HONO permeation source was recorded over a 12 hour period using NO_x measured by the differential photolysis analyser (the most sensitive measurement available) as a proxy for NO, NO_2, and HONO. The stability was found to be ±0.01 ppb h^{-1}, with a standard deviation of 0.4 ppb. The uncertainty in the HONO source is determined by a combination of the accuracy of the NO, NO_2, and NO_y measurements and their respective calibrations. The NO calibration uncertainty, due to MFC flows and standard gas accuracy is 5%, similarly for the CAPS NO_2 and Thermo 42i TL NO_y. This results in an overall uncertainty in [HONO] of 8.7%.

In Fig. 2 the observed conversion of HONO, that is the difference between HONO conversion by the 385 and 395 nm lamps, is shown. As can be seen HONO conversion is consistently 6.54 ± 0.21 % more at 385nm than 395 nm. The fact that the 'apparent HONO conversion' (HONO CE_{385} –HONO CE_{395} in Eq. 1) is constant as a function of HONO means that the determination of

Atmos. Meas. Tech. Discuss., doi:10.5194/amt-2016-17, 2016
Manuscript under review for journal Atmos. Meas. Tech.
Published: 25 January 2016

Atmospheric Measurement Techniques Discussions

[HONO] should be a linear function of the difference in $NO_2^{\dagger}$ signal at 385 and 395 nm. This apparent HONO conversion determines the limit of detection, which is the ability of the analyser to discriminate the difference in signal arising from photolysis at the two different wavelengths from photon counting noise. With an apparent conversion of 6.54 ± 0.21 % the LOD with a sensitivity of 6.4 cps/ppt is 40 ppt min^{-1}. The uncertainty in the apparent conversion is a combination of the uncertainty in the HONO source, and in the NO_2 conversion efficiencies of the two lamps. This results in an overall uncertainty of 12.2%.

The effect of the back reaction of OH + NO, reforming HONO, before detection of NO, thus reducing the NO signal in the NO_x/HONO measurement in the presence of HONO was calculated using a box model in FACSMILE kinetic modelling software (MCPA Software Ltd.). Kinetic data for O_x, HO_x, and NO_x reactions taken from IUPAC Evaluated Kinetic Data (Atkinson et al., 2004). The residence time between an air sample exiting the photolysis cell and entering the high vacuum of the NO analyser through the ~ 25 cm of ¼ inch PFA tubing is 0.11 s. The air sample is a mixture of mostly NO, O_3, OH, and unconverted NO_2. The absence of UV irradiation results in chemistry analogous to night-time NO_x chemistry with the addition of a significant OH source. The box model was initiated with NO, NO_3, O_3, and OH concentrations calculated to be at the outlet of the photolysis cell at each of the eight calibration points shown previously. The interference from the OH + NO reaction was determined as the decrease in [NO] during the 0.11 s residence time as a percentage of measured [HONO]. The discrepancy was calculated to vary linearly with [HONO] from -0.97 to -2.10 %, with differences between lamps well within the accuracy of the calibration. The degree of interference from OH in NO_2 and HONO determination was found to be a function of k([OH]+[NO]) on the timescale here (0.11 s). Reducing the residence time after the photolysis cell would reduce the error in HONO and NO_2 (in the presence of HONO). Conversely, a system with a suitably long residence time between the photolysis cell and detector may experience little-to-no HONO interference as the OH + NO back reaction begins to dominate. There is of course a trade off in that the data must be corrected for ambient ozone affecting the NO:NO_2 ratio. It is important to note that there can never be any negative interference in NO_2 caused by the presence of HONO, only positive or none.

Atmos. Meas. Tech. Discuss., doi:10.5194/amt-2016-17, 2016
Manuscript under review for journal Atmos. Meas. Tech.
Published: 25 January 2016

Outside of calibration the effect of the OH back reaction with NO is likely to be less significant due to the presence of volatile organic compounds (VOCs) which also react with OH with comparable rates to NO. It is therefore difficult to know the absolute HONO conversion of each UV-LED without very accurate OH reactivity/VOC concentration measurements. Due to these unknowns, it would not be possible to correct the NO_2 signal for HONO interference as might be hoped.

3 Results and discussion

The pHONO instrument was evaluated in an atmospheric simulation chamber (section 3.1) and compared in the field side-by-side with LOPAP (section 3.2).

3.1 Chamber measurements

The Highly Instrumented Reactor for Atmospheric Chemistry (HIRAC) is a simulation chamber facility based at the School of Chemistry, University of Leeds (Glowacki et al., 2007a). HIRAC is a cylindrical stainless steel chamber with a total volume of ~2.25 m^3, containing four fans for mixing throughout the chamber, and with a total mixing time of ~60 s. The stainless steel structure of HIRAC allows for pressure dependent experiments to be carried out, over the range of ~10 – 1000 mbar. Numerous sample ports are located around the chamber allowing the attaching of instruments or introduction of gas. A multi pass Fourier Transform - Infrared (FT-IR) instrument (Bruker IFS/66, 128.52 m path length) is present to allow spectra of the gas within the chamber to be taken (Glowacki et al., 2007b). HIRAC is also capable of operating over a range of temperatures (-40 to 70°C).

Experiments were carried out at ambient temperature (20 ^{o}C) and pressure (1000 mbar), whilst the chamber was kept dark. HIRAC was filled with 80 % N_2 (BOC, UHP, 99.998 %) and 20 % O_2 (BOC) before HONO was synthesised external to the chamber following a modified procedure described previously by (Taira and Kanda, 1990). A 1 % aqueous sodium nitrite solution was added dropwise to a 30 % aqueous solution of sulfuric acid. The resulting reaction (R6) produces HONO, which was added directly to the chamber via a continuous flow of N_2 over the reaction mixture. This is analogous to the permeation source however, side products need not be considered due to the direct HONO measurement afforded by FT-IR.

Atmos. Meas. Tech. Discuss., doi:10.5194/amt-2016-17, 2016
Manuscript under review for journal Atmos. Meas. Tech.
Published: 25 January 2016

Atmospheric Measurement Techniques Discussions

$$2NaNO_2 + H_2SO_4 \rightarrow 2HONO + Na_2HSO_4 \quad \text{(R6)}$$

FT-IR spectra were taken at 60 second intervals with a spectral resolution of 1 cm^{-1}, whilst the differential photolysis analyser sampled from the chamber. Dilution of the HONO, NO, NO_2 mixture was achieved by partial evacuation of the chamber and subsequent refilling with synthetic air (N_2/O_2). The average HONO concentration determined from the average of two distinct absorbance lines at 1264 cm^{-1} (*trans*-HONO, Q-branch) and 853 cm^{-1} (*cis*-HONO, Q-Branch) in the FT-IR using absorptivity data taken from University of Wuppertal internal FT-IR cross-section database, courtesy of I. Bejan via personal communication. The absorptivity data were $7.60\times10^{-4} \pm 2.90\times10^{-5}$ ppm^{-1} m^{-1} (1264 cm^{-1}, *tans*-HONO) and $5.48\times10^{-4} \pm 2.60\times10^{-5}$ ppm^{-1} m^{-1} (853 cm^{-1}, *cis*-HONO). Some of the spectra used in quantification are shown in Fig. 3.

Figure 4 shows the strong, positive correlation between the HONO measured by differential photolysis and by FT-IR within the HIRAC chamber up to ~ 150 ppbV, deviating at higher mixing ratios.

Figure 4 shows that at lower HONO mixing ratios, < 150 ppb, there is better agreement between the pHONO and FT-IR measurements, whereas the response of the differential photolysis technique appears to be suppressed at high [HONO]. This is a result of how a photolytic converter operates as expressed by Eq. (3) (Ryerson et al., 2000). Here t is the residence time within the photolysis cell and k[Ox] is the concentration and rate constant of any oxidant that reacts with NO. Typically this would be ozone, however, OH formed from HONO photolysis must also be considered.

$$CE = \left[\frac{jt}{jt+k[\mathrm{Ox}]t}\right]\left[1 - exp^{(-jt-k[\mathrm{Ox}]t)}\right] \quad (3)$$

Having two LEDs with different HONO absorption overlap results in two values for j(HONO). Using the $j(NO_2)$ values already found (1.3 & 1.7 s^{-1}) as an easily determined proxy for j(HONO) the change in conversion with oxidant concentration can be approximated.

Figure 5 shows how the percentage conversion of any precursor that dissociates to NO, in this case HONO and NO_2, changes with increasing oxidant concentration. In the case of O_3 the total conversion decreases linearly with increasing [Ox], whilst the difference between the two

Atmos. Meas. Tech. Discuss., doi:10.5194/amt-2016-17, 2016
Manuscript under review for journal Atmos. Meas. Tech.
Published: 25 January 2016

Atmospheric Measurement Techniques Discussions

remains constant (9%). Conversely, with OH, conversion decays exponentially in total, and as a difference between two LEDs of different *j*. This effect can be seen clearly above 150 ppbV HONO in Fig. 4. Below 150 ppbV a constant difference in conversion of 6.54% is a reasonable approximation.

The high HONO mixing ratios within HIRAC, necessary to be detected by FT-IR (LOD ~ 40 ppb), were several orders of magnitude higher than would be expected in the atmosphere where ppt (Beine et al., 2006; Ren et al., 2010; Zhang et al., 2009, 2012) to low ppb (Acker et al., 2006; Febo et al., 1996; Hendrick et al., 2014; Kanaya et al., 2007; Stutz, 2004) are typical. Thus, this non-linearity at high [HONO] is unlikely to pose a serious limitation of the differential photolysis method, with the possible exception of areas with very high NO_x backgrounds. This could be partially mitigated by having greater photolysis power at 385 nm, in combination with moving to shorter wavelengths with better overlap with the HONO absorption cross-section. It is clear in Fig. 1 that the 385 nm UV-LED has significantly lower light output than at 395 nm; this is reflected in their respective NO_2 conversion efficiencies (72.9 and 81.3%). Alternatively, separate 385 and 395 nm converters can be employed working in parallel, thus doubling the number of UV-LEDs and doubling the photolysis power at each respective wavelength. This would also allow for fast measurement simultaneously i.e. 1 Hz or faster. Alternatively, the lower conversion efficiency at high [HONO] could be calibrated for, though as shown in the following section, in typical atmospheric conditions no calibration or correction was required.

3.2 Field measurements

The Weybourne Atmospheric Observatory (Penkett et al., 1999) is a regional GAW station located on the North Norfolk coast, UK (52°57'01.5"N 1°07'19"E). The WAO has a long history of atmospheric measurements stretching back to its inception in 1994. During summer 2015, the WAO was host to the Integrated Chemistry of Ozone in the Atmosphere (ICOZA) campaign, ostensibly measuring ozone production rates. As part of the campaign a Long Path Absorption Photometer (LOPAP-03, QUMA GmbH) (Heland et al., 2001) was deployed in order to measure HONO. Alongside the LOPAP, the NO, NO_2, HONO (Differential photolysis) instrument described in section 2.1 measured concurrently at a 1 minute time resolution.

Atmos. Meas. Tech. Discuss., doi:10.5194/amt-2016-17, 2016
Manuscript under review for journal Atmos. Meas. Tech.
Published: 25 January 2016

Atmospheric Measurement Techniques Discussions

During the ICOZA campaign, a high variation of HONO concentrations (up to ~ 500 ppt) was observed by the LOPAP on the 1st and 2nd of July providing an ideal opportunity for comparison between the two methods. The pHONO was deployed with replacement UV-LEDs with greater output. Both the 385 and 395 nm lamps had the same photon flux, indicated by identical NO_2 conversion efficiencies (~ 89%), in the expectation that better HONO conversion, and therefore sensitivity, would be achieved. The estimated increase in overlap with the HONO adsorption spectrum of the new 385 nm LED was 45% compared to 30% calculated for the original LED. Thus lamps were installed as-is without calibration to mitigate the fall in output over time that affects the LEDs, particularly the 385 nm LED. The decreasing output is believed to be a result of the power control circuitry of the LEDs which does not limit the current draw immediately after power is supplied, only after a few seconds. This means every time the lamp is switched on it outputs its maximum (with corresponding heat), which, when used in a 30 s^{-1} switching mode as here shortens the life considerably.

The pHONO instrument sampled from an inlet box (also housing a NO_y converter) located ~ 4 m from ground level on the sampling tower at Weybourne. The sample point was connected to the instrument by a 12 m ¼ inch PFA line (Swagelok) which was shared by the CAPS NO_2 instrument, thus the flowrate was ~ 3 standard L min^{-1}, resulting in a residence time of ~ 3 seconds. The LOPAP instrument, which has its own inlet, sampled from the roof of a specially converted van located 20 m away upslope. Consequently, both instruments sampled at a similar height and there was clear, unobstructed line-of-sight between them. The pHONO inlet was only ~1 m above the Weybourne observatory roof which may have contributed to the turbulent dynamics observed in the data. The pHONO instrument was calibrated for sensitivity in ambient air twice nightly at 00:00 and 04:00 am; NO offset was taken between these times. NO_2 conversion efficiencies were determined in zero air once per week. Limits of detection were 1.5 ppt min^{-1} and 1.9 ppt min^{-1} for NO and NO_2, respectively. The LOPAP was operated and calibrated according to the standard procedures described in Kleffmann and Wiesen, (2008), with a detection limit of 3 pptV and time resolution of 5 minutes. Zero measurements using high purity N_2 (N5 grade, BOC) were performed every 12 hours on the LOPAP.

Figure 6 shows the HONO time series from both the LOPAP and pHONO instruments during three days of high HONO measurements.

Atmos. Meas. Tech. Discuss., doi:10.5194/amt-2016-17, 2016
Manuscript under review for journal Atmos. Meas. Tech.
Published: 25 January 2016

There is reasonable agreement between the established LOPAP method of HONO measurement and that provided by the pHONO instrument without correction or calibration (Fig. 6). During the high ozone and high HONO events observed on the 1st and 2nd especially there is very good agreement between the two. Gaps in the data represent times where the pHONO limit of determination was reached; where there are too few points in the averaging window after statistical analysis of the data to be meaningful. This is because in real atmospheric conditions the pHONO instrument is hampered by the time resolution that data is collected i.e. if there is strong turbulence, meaning the NO_2 or HONO concentration varies rapidly on a timescale shorter than that at which data is collected, then wide scatter is observed as was the case at Weybourne. Strong boundary layer transport meant that NO_2 measurement varied up to 1.5 ppb in a minute. This is because of the way the data must be processed by interpolating between measurements and subtraction of the 395 nm signal form the 385 nm signal. Decreasing the time between photolysis switching (from 30 s) would obviously decrease this effect, but ultimately, separate 385 nm (or lower) and 395 nm analyser channels are required. Consequently the data analysis routine for the pHONO data includes tests for the variability of the data, discarding points which show >5% variation from the subsequent point. Data failing this test is discarded and results in gaps; this is the effective limit of determination. The data is then treated with a robust-LOESS (Cleveland, 1979) algorithm to remove extreme values. The gaps in the time series of LOPAP (Fig 5) were due to the removal of zero measurements and false spikes due to bubbles passing the detector.

Figure 7 demonstrates the level of agreement in the measured HONO concentration by the LOPAP and pHONO methods from 1st and 2nd July. From Fig. 7, the observed correlation (r^2 of 0.68) suggests the replacement UV-LEDs had the desired effect without the application of corrections for the HONO conversion efficiency. The slope of ~ 0.91 suggests that the new 385 nm lamp was able to convert the majority of HONO. The discrepancy suggests that ~ 9% of HONO was converted by the 395 nm lamp. The scatter evident in Fig. 7 at low mixing ratios may be due to atmospheric dynamic effects resulting in a rapidly changing NO_2 background on timescales faster than the response of the instrument (30 s^{-1}). A positive 5 pptV positive intercept indicates a small systematic off-set in the pHONO instrument.

Accuracy and uncertainty in unstable conditions could be improved by measuring at the two different wavelengths concurrently, rather than consecutively. In the same way photolytic NO_2 measurement is improved by measuring concurrently with NO, rather than consecutively. This would require three chemiluminescent analysers in parallel, with two photolytic converters. However, in ambient indoor air quality monitoring, where HONO is seen as increasingly important (Gligorovski, 2016), a simple single channel, dual wavelength design might be appropriate and useful.

4 Conclusions

An instrument for *in*-situ determination of HONO photolytically has been developed, characterized and deployed in the field as a proof-of-concept. During an atmospheric simulation chamber comparison, the HONO measured corresponded well with FT-IR measurement. During field tests the photolytic HONO instrument agreed reasonably well with the established LOPAP instrument, though the limitations of having a 2-channel sequential measurement were apparent at times; this would be easily overcome in a 3-channel concurrent system. Calibration would gain from a pure HONO source; currently the pHONO calibration requires an independent, direct NO_2 measurement and NO_y measurement.

Acknowledgments

The authors would like to express their gratitude to Dr Marty Buhr or Air Quality Design inc. their support, and Dr Lisa Whalley of Leeds for Spectral Radiometer/calibration equipment. Dr Iusti Bejan, formerly of Leeds, receives thanks for his invaluable guidance in HONO quantification within HIRAC. The financial support of the Engineering and Physical Sciences Research Council (ESPRC) for the studentship of Charlotte Brumby, and the financial support of NCAS, the National Centre for Atmospheric Science, and of NERC, the Natural Environmental Research Council for supporting the studentship of Chris Reed are gratefully acknowledged.

References

Acker, K., Febo, A., Trick, S., Perrino, C., Bruno, P., Wiesen, P., Möller, Wieprecht, W., Auel, R., Giusto, M., Geyer, A., Platt, U. and Allegrini, I.: Nitrous acid in the urban area of Rome, Atmos. Environ., 40(17), 3123–3133, doi:10.1016/j.atmosenv.2006.01.028, 2006.

Acker, K., Möller, D., Auel, R., Wieprecht, W. and Kalaß, D.: Concentrations of nitrous acid, nitric acid, nitrite and nitrate in the gas and aerosol phase at a site in the emission zone during ESCOMPTE 2001 experiment, Atmos. Res., 74(1-4), 507–524, doi:10.1016/j.atmosres.2004.04.009, 2005.

Atkinson, R., Baulch, D. L., Cox, R. A., Crowley, J. N., Hampson, R. F., Hynes, R. G., Jenkin, M. E., Rossi, M. J. and Troe, J.: Evaluated kinetic and photochemical data for atmospheric chemistry: Volume I - gas phase reactions of O_x, HO_x, NO_x and SO_x species, Atmos. Chem. Phys., 4(6), 1461–1738, doi:10.5194/acp-4-1461-2004, 2004.

Beine, H., Colussi, A. J., Amoroso, A., Esposito, G., Montagnoli, M. and Hoffmann, M. R.: HONO emissions from snow surfaces, Environ. Res. Lett., 3(4), 045005, doi:10.1088/1748-9326/3/4/045005, 2008.

Beine, H. J., Amoroso, A., Domine, F., King, M. D., Nardino, M., Ianniello, A. and France, J. L.: Surprisingly small HONO emissions from snow surfaces at Browning Pass, Antarctica, Atmos. Chem. Phys., 6, 2569–2580, doi:10.5194/acp-6-2569-2006, 2006.

Bröske, R., Kleffmann, J. and Wiesen, P.: Heterogeneous conversion of NO2 on secondary organic aerosol surfaces: A possible source of nitrous acid (HONO) in the atmosphere?, Atmos. Chem. Phys., 3(3), 469–474, doi:10.5194/acp-3-469-2003, 2003.

Buhr, M.: Measurement of NO2 in ambient air using a solid-state photolytic converter, in Symposium on Air Quality Measurement Methods and Technology 2004. 20 - 22 April 2004, pp. 165–171, Cary, NC, USA., 2004.

Buhr, M.: Solid-state light source photolytic nitrogen dioxide converter, US 7238328 B2, 3 July 2007.

Clemitshaw, K. C.: A Review of Instrumentation and Measurement Techniques for Ground-Based and Airborne Field Studies of Gas-Phase Tropospheric Chemistry, Crit. Rev. Environ. Sci. Technol., 34(1), 1–108, doi:10.1080/10643380490265117, 2004.

Cleveland, W. S.: Robust Locally Weighted Regression and Smoothing Scatterplots, J. Am. Stat. Assoc., 74(368), 829–836, doi:10.2307/2286407, 1979.

Elshorbany, Y. F., Kurtenbach, R., Wiesen, P., Lissi, E., Rubio, M., Villena, G., Gramsch, E., Rickard, A. R., Pilling, M. J. and Kleffmann, J.: Oxidation capacity of the city air of Santiago, Chile, Atmos. Chem. Phys. Discuss., 8(6), 19123–19171, doi:10.5194/acpd-8-19123-2008, 2008.

Febo, A., Perrino, C. and Allegrini, I.: Measurement of Nitrous Acid in Milan , Italy, By Doas and Diffusion Denuders, Atmos. Environ., 30(21), 3599–3609, doi:10.1016/1352-2310(96)00069-6, 1996.

Febo, A., Perrino, C. and Cortiello, M.: A denuder technique for the measurement of nitrous acid in urban atmospheres, Atmos. Environ. Part A. Gen. Top., 27(11), 1721–1728, doi:10.1016/0960-1686(93)90235-Q, 1993.

Febo, A., Perrino, C., Gherardi, M. and Sparapani, R.: Evaluation of a High-Purity and High-Stability Continuous Generation System for Nitrous Acid, Environ. Sci., 29(9), 2390–2395, doi:10.1021/es00009a035, 1995.

Fehsenfeld, F. C., Dickerson, R. R., Hobler, G., Luke, W. T., Nunnermacker, L. J., Roberts, J.

M., Curran, C. M., Eubank, C. S., Fahey, D. W., Mindplay, P. C. and Pickering, K. E.: A Ground-Based Intercomparison of NO, NOx, and NOy Measurement Techniques, J. Geophys. Res., 92(7), 710–722, doi:10.1029/JD092iD12p14710, 1987.

Finlayson-Pitts, B. J., Wingen, L. M., Sumner, A. L., Syomin, D. and Ramazan, K. A.: The heterogeneous hydrolysis of NO2 in laboratory systems and in outdoor and indoor atmospheres: An integrated mechanism, Phys. Chem. Chem. Phys., 5(2), 223–242, doi:10.1039/B208564J, 2003.

Gligorovski, S.: Nitrous acid (HONO): An emerging indoor pollutant, J. Photochem. Photobiol. A Chem., 314, 1–5, doi:10.1016/j.jphotochem.2015.06.008, 2016.

Glowacki, D. R., Goddard, A., Hemavibool, K., Malkin, T. L., Commane, R., Anderson, F., Bloss, W. J., Heard, D. E., Ingham, T., Pilling, M. J. and Seakins, P. W.: Design of and initial results from a highly instrumented reactor for atmospheric chemistry (HIRAC), Atmos. Chem. Phys. Discuss., 7, 10687–10742, doi:10.5194/acpd-7-10687-2007, 2007a.

Glowacki, D. R., Goddard, A. and Seakins, P. W.: Design and performance of a throughput-matched, zero-geometric-loss, modified three objective multipass matrix system for FTIR spectrometry, Appl. Opt., 46(32), 7872–7883, doi:10.1364/AO.46.007872, 2007b.

Gutzwiller, L., Arens, F., Baltensperger, U., Gäggeler, H. W. and Ammann, M.: Significance of semivolatile diesel exhaust organics for secondary HONO formation, Environ. Sci. Technol., 36(4), 677–682, doi:10.1021/es015673b, 2002.

Heland, J., Kleffmann, J., Kurtenbach, R. and Wiesen, P.: A new instrument to measure gaseous nitrous acid (HONO) in the atmosphere, Environ. Sci. Technol., 35(15), 3207–3212, doi:10.1021/es000303t, 2001.

Hendrick, F., Clémer, K., Wang, P., De Mazière, M., Fayt, C., Gielen, C., Hermans, C., Ma, J. Z., Pinardi, G., Stavrakou, T., Vlemmix, T. and Van Roozendael, M.: Four years of ground-based MAX-DOAS observations of HONO and NO2 in the Beijing area, Atmos. Chem. Phys., 14(2), 765–781, doi:10.5194/acp-14-765-2014, 2014.

Ianniello, A., Beine, H. J., Landis, M. S., Stevens, R. K., Esposito, G., Amoroso, A. and Allegrini, I.: Comparing field performances of denuder techniques in the high Arctic, Atmos. Environ., 41(8), 1604–1615, doi:10.1016/j.atmosenv.2006.10.040, 2007.

Kanaya, Y., Cao, R., Akimoto, H., Fukuda, M., Komazaki, Y., Yokouchi, Y., Koike, M., Tanimoto, H., Takegawa, N. and Kondo, Y.: Urban photochemistry in central Tokyo: 1. Observed and modeled OH and HO_2 radical concentrations during the winter and summer of 2004, J. Geophys. Res., 112(D21), D21312, doi:10.1029/2007JD008670, 2007.

Kebabian, P. L., Herndon, S. C. and Freedman, A.: Detection of nitrogen dioxide by cavity attenuated phase shift spectroscopy, Anal. Chem., 77(2), 724–728, doi:10.1021/ac048715y, 2005.

Kebabian, P. L., Wood, E. C., Herndon, S. C. and Freedman, A.: A practical alternative to chemiluminescence-based detection of nitrogen dioxide: Cavity attenuated phase shift spectroscopy, Environ. Sci. Technol., 42(16), 6040–6045, doi:10.1021/es703204j, 2008.

Kim, S., VandenBoer, T. C., Young, C. J., Riedel, T. P., Thornton, J. A., Swarthout, B., Sive, B.,

Lerner, B. M., Gilman, J. B., Warneke, C., Roberts, J. M., Guenther, A., Wagner, N. L., Dubé, W. P., Williams, E. J. and Brown, S. S.: The primary and recyling sources of OH during the NACHTT-2011 campaign: HONO as an important OH primary source in the wintertime, J. Geophys. Res. Atmos., 119(11), 6886–6896, doi:10.1002/2013JD021272.Received, 2014.

Kirchstetter, T. W., Harley, R. A. and Littlejohn, D.: Measurement of Nitrous Acid in Motor Vehicle Exhaust, Environ. Sci. Technol., 30(9), 2843–2849, doi:10.1021/es960135y, 1996.

Kleffmann, J.: Daytime sources of nitrous acid (HONO) in the atmospheric boundary layer, ChemPhysChem, 8(8), 1137–1144, doi:10.1002/cphc.200700016, 2007.

Kleffmann, J., Lörzer, J. C., Wiesen, P., Kern, C., Trick, S., Volkamer, R., Rodenas, M. and Wirtz, K.: Intercomparison of the DOAS and LOPAP techniques for the detection of nitrous acid (HONO), Atmos. Environ., 40(20), 3640–3652, doi:10.1016/j.atmosenv.2006.03.027, 2006.

Kleffmann, J., Villena Tapia, G., Bejan, I., Kurtenbach, R. and Wiesen, P.: NO2 Measurement Techniques: Pitfalls and New Developments, edited by I. Barnes and K. J. Rudziński, NATO Sci. Peace Secur. Ser. C Environ. Secur., 120(2), 15–28, doi:10.1007/978-94-007-5034-0, 2013.

Kleffmann, J. and Wiesen, P.: Technical note: Quantification of interferences of wet chemical HONO LOPAP measurements under simulated polar conditions, Atmos. Chem. Phys., 8(22), 6813–6822, doi:10.5194/acp-8-6813-2008, 2008.

Kurtenbach, R., Becker, K. H., Gomes, J. A. G., Kleffmann, J., Lörzer, J. C., Spittler, M., Wiesen, P., Ackermann, R., Geyer, A. and Platt, U.: Investigations of emissions and heterogeneous formation of HONO in a road traffic tunnel, Atmos. Environ., 35(20), 3385–3394, doi:10.1016/S1352-2310(01)00138-8, 2001.

Lammel, G. and Cape, J. N.: Nitrous acid and nitrite in the atmosphere, Chem. Soc. Rev., 25(5), 361, doi:10.1039/cs9962500361, 1996.

Lee, B. H., Wood, E. C., Zahniser, M. S., McManus, J. B., Nelson, D. D., Herndon, S. C., Santoni, G. W., Wofsy, S. C. and Munger, J. W.: Simultaneous measurements of atmospheric HONO and NO2 via absorption spectroscopy using tunable mid-infrared continuous-wave quantum cascade lasers, Appl. Phys. B Lasers Opt., 102(2), 417–423, doi:10.1007/s00340-010-4266-5, 2011.

Lee, J. D., Moller, S. J., Read, K. A., Lewis, A. C., Mendes, L. and Carpenter, L. J.: Year-round measurements of nitrogen oxides and ozone in the tropical North Atlantic marine boundary layer, J. Geophys. Res., 114, doi:10.1029/2009JD011878, 2009.

Lee, J. D., Whalley, L. K., Heard, D. E., Stone, D., Dunmore, R. E., Hamilton, J. F., Young, D. E., Allan, J. D., Laufs, S. and Kleffmann, J.: Detailed budget analysis of HONO in central London reveals a missing daytime source., 2015.

Levy II, H.: Photochemistry of minor constituents in the troposphere, Planet. Space Sci., 21(4), 575–591, doi:10.1016/0032-0633(73)90071-8, 1973.

Levy, M., Zhang, R., Zheng, J., Zhang, A. L., Xu, W., Gomez-Hernandez, M., Wang, Y. and Olaguer, E.: Measurements of nitrous acid (HONO) using ion drift-chemical ionization mass spectrometry during the 2009 SHARP field campaign, Atmos. Environ., 94(2), 231–240, doi:10.1016/j.atmosenv.2014.05.024, 2014.

Markovic, M. Z., VandenBoer, T. C. and Murphy, J. G.: Characterization and optimization of an online system for the simultaneous measurement of atmospheric water-soluble constituents in the gas and particle phases, J. Environ. Monit., 14(7), 1872, doi:10.1039/c2em00004k, 2012.

Oswald, R., Behrendt, T., Ermel, M., Wu, D., Su, H., Cheng, Y., Breuninger, C., Moravek, A., Mougin, E., Delon, C., Loubet, B., Pommerening-Röser, A., Sörgel, M., Pöschl, U., Hoffmann, T., Andreae, M. O., Meixner, F. X. and Trebs, I.: HONO emissions from soil bacteria as a major source of atmospheric reactive nitrogen., Science, 341(6151), 1233–5, doi:10.1126/science.1242266, 2013.

Penkett, S. a., Plane, J. M. C., Comes, F. J., Clemitshaw, K. C. and Coe, H.: The Weybourne Atmospheric Observatory, J. Atmos. Chem., 33(2), 107–110, doi:10.1023/A:1026428102821, 1999.

Pollack, I. B., Lerner, B. M. and Ryerson, T. B.: Evaluation of ultraviolet light-emitting diodes for detection of atmospheric NO2 by photolysis - chemiluminescence, J. Atmos. Chem., 65(2-3), 111–125, doi:10.1007/s10874-011-9184-3, 2011.

Pusede, S. E., Gentner, D. R., Wooldridge, P. J., Browne, E. C., Rollins, A. W., Min, K.-E., Russell, A. R., Thomas, J., Zhang, L., Brune, W. H., Henry, S. B., DiGangi, J. P., Keutsch, F. N., Harrold, S. A., Thornton, J. A., Beaver, M. R., St. Clair, J. M., Wennberg, P. O., Sanders, J., Ren, X., VandenBoer, T. C., Markovic, M. Z., Guha, A., Weber, R., Goldstein, A. H. and Cohen, R. C.: On the temperature dependence of organic reactivity, nitrogen oxides, ozone production, and the impact of emission controls in San Joaquin Valley, California, Atmos. Chem. Phys., 14(7), 3373–3395, doi:10.5194/acp-14-3373-2014, 2014.

Reed, C., Evans, M. J., Di Carlo, P., Lee, J. D. and Carpenter, L. J.: Interferences in photolytic NO2 measurements: explanation for an apparent missing oxidant?, Atmos. Chem. Phys. Discuss., 15(20), 28699–28747, doi:10.5194/acpd-15-28699-2015, 2015.

Ren, X., Gao, H., Zhou, X., Crounse, J. D., Wennberg, P. O., Browne, E. C., LaFranchi, B. W., Cohen, R. C., McKay, M., Goldstein, A. H. and Mao, J.: Measurement of atmospheric nitrous acid at Blodgett Forest during BEARPEX2007, Atmos. Chem. Phys., 10(13), 6501, doi:10.5194/acp-10-6283-2010, 2010.

Ren, X., Sanders, J. E., Rajendran, a., Weber, R. J., Goldstein, a. H., Pusede, S. E., Browne, E. C., Min, K. E. and Cohen, R. C.: A relaxed eddy accumulation system for measuring vertical fluxes of nitrous acid, Atmos. Meas. Tech., 4(10), 2093–2103, doi:10.5194/amt-4-2093-2011, 2011.

Roberts, J. M., Veres, P., Warneke, C., Neuman, J. A., Washenfelder, R. A., Brown, S. S., Baasandorj, M., Burkholder, J. B., Burling, I. R., Johnson, T. J., Yokelson, R. J. and De Gouw, J.: Measurement of HONO, HNCO, and other inorganic acids by negative-ion proton-transfer chemical-ionization mass spectrometry (NI-PT-CIMS): Application to biomass burning emissions, Atmos. Meas. Tech., 3, 981–990, doi:10.5194/amt-3-981-2010, 2010.

Ródenas, M., Muñoz, A., Alacreu, F., Brauers, T., Dorn, H.-P., Kleffmann, J. and Bloss, W.: Assessment of HONO Measurements: The FIONA Campaign at EUPHORE, in Disposal of Dangerous Chemicals in Urban Areas and Megacities, NATO Science for Peace & Security Series C: Environmental Security, pp. 45–58., 2013.

Ryerson, T. B., Williams, E. J. and Fehsenfeld, F. C.: An efficient photolysis system for fast-response NO2 measurements, J. Geophys. Res., 105(2), 26,447–26,461, doi:10.1029/2000JD900389, 2000.

Sadanaga, Y., Fukumori, Y., Kobashi, T., Nagata, M., Takenaka, N. and Bandow, H.: Development of a selective light-emitting diode photolytic NO2 converter for continuously measuring NO2 in the atmosphere, Anal. Chem., 82(2), 9234–9239, doi:10.1021/ac101703z, 2010.

Sadanaga, Y., Suzuki, K., Yoshimoto, T. and Bandow, H.: Direct measurement system of nitrogen dioxide in the atmosphere using a blue light-emitting diode induced fluorescence technique., Rev. Sci. Instrum., 85(6), 064101, doi:10.1063/1.4879821, 2014.

Sander, S. P., Golden, D. M., Kurylo, M. J., Moorgat, G. K., Keller-Rudek, H., Wine, P. H., Ravishankara, A. R., Kolb, C. E., Molina, M. J., Finlayson-Pitts, B. J., Huie, R. E., and Orkin, V. L.: Chemical Kinetics and Photochemical Data for Use in Atmospheric Studies, Evaluation No. 17, JPL Publication 10-6, Jet Propulsion Laboratory, Pasadena, USA, available at: http://jpldataeval.jpl.nasa.gov (last access: 3 December 2015), 2011Sörgel, M., Regelin, E., Bozem, H., Diesch, J.-M., Drewnick, F., Fischer, H., Harder, H., Held, A., Hosaynali-Beygi, Z., Martinez, M. and Zetzsch, C.: Quantification of the unknown HONO daytime source and its relation to NO2, Atmos. Chem. Phys., 11(20), 10433–10447, doi:10.5194/acp-11-10433-2011, 2011.

Spataro, F. and Ianniello, A.: Sources of atmospheric nitrous acid: State of the science, current research needs, and future prospects, J. Air Waste Manage. Assoc., 64(11), 1232–1250, doi:10.1080/10962247.2014.952846, 2014.

Stutz, J.: Relative humidity dependence of HONO chemistry in urban areas, J. Geophys. Res., 109(D3), D03307, doi:10.1029/2003JD004135, 2004.

Stutz, J., Oh, H. J., Whitlow, S. I., Anderson, C., Dibb, J. E., Flynn, J. H., Rappenglück, B. and Lefer, B.: Simultaneous DOAS and mist-chamber IC measurements of HONO in Houston, TX, Atmos. Environ., 44(33), 4090–4098, doi:10.1016/j.atmosenv.2009.02.003, 2010.

Su, H., Cheng, Y., Oswald, R., Behrendt, T., Trebs, I., Meixner, F. X., Andreae, M. O., Cheng, P., Zhang, Y. and Pöschl, U.: Soil nitrite as a source of atmospheric HONO and OH radicals., Science, 333(6049), 1616–8, doi:10.1126/science.1207687, 2011.

Taira, M. and Kanda, Y.: Continuous generation system for low-concentration gaseous nitrous acid, Anal. Chem., 633(15), 630–633, doi:10.1021/ac00205a018, 1990.

Vandenboer, T. C., Markovic, M. Z., Sanders, J. E., Ren, X., Pusede, S. E., Browne, E. C., Cohen, R. C., Zhang, L., Thomas, J., Brune, W. H. and Murphy, J. G.: Evidence for a nitrous acid (HONO) reservoir at the ground surface in Bakersfield, CA, during CalNex 2010, J. Geophys. Res. Atmos., 119, 9093–9106, doi:10.1002/2013JD020971.Received, 2014.

Villena, G., Bejan, I., Kurtenbach, R., Wiesen, P. and Kleffmann, J.: Development of a new Long Path Absorption Photometer (LOPAP) instrument for the sensitive detection of NO2 in the atmosphere, Atmos. Meas. Tech., 4, 1663–1676, doi:10.5194/amt-4-1663-2011, 2011a.

Villena, G., Bejan, I., Kurtenbach, R., Wiesen, P. and Kleffmann, J.: Interferences of commercial NO_2 instruments in the urban atmosphere and in a smog chamber, Atmos. Meas. Tech., 5(1),

149–159, doi:10.5194/amt-5-149-2012, 2012.

Villena, G., Kleffmann, J., Kurtenbach, R., Wiesen, P., Lissi, E., Rubio, M. A., Croxatto, G. and Rappenglück, B.: Vertical gradients of HONO, NOx and O3 in Santiago de Chile, Atmos. Environ., 45(23), 3867–3873, doi:10.1016/j.atmosenv.2011.01.073, 2011b.

Weber, B., Wu, D., Tamm, A., Ruckteschler, N., Rodríguez-Caballero, E., Steinkamp, J., Meusel, H., Elbert, W., Behrendt, T., Sörgel, M., Cheng, Y., Crutzen, P. J., Su, H. and Pöschl, U.: Biological soil crusts accelerate the nitrogen cycle through large NO and HONO emissions in drylands, Proc. Natl. Acad. Sci., 112(50), 201515818, doi:10.1073/pnas.1515818112, 2015.

Williams, E. J., Baumann, K., Roberts, J. M., Bertman, S. B., Norton, R. B., Fehsenfeld, F. C., Sprinston, S. R., Nunnermacker, L. J., Newman, L., Olszyna, K., Meagher, J. F., Hartsell, B., Edgerton, E. S., Pearson, J. R. and Rodgers, M. O.: Intercomparison of ground-based NOy measurement techniques, J. Geophys. Res., 103(17), 22261–22280, doi:10.1029/98JD00074, 1998.

Yang, X., Cox, R. A., Warwick, N. J., Pyle, J. A., Carver, G. D., O'Connor, F. M. and Savage, N. H.: Tropospheric bromine chemistry and its impacts on ozone: A model study, J. Geophys. Res., 110(D23), D23311, doi:10.1029/2005JD006244, 2005.

Zhang, N., Zhou, X., Bertman, S., Tang, D., Alaghmand, M., Shepson, P. B. and Carroll, M. a.: Measurements of ambient HONO concentrations and vertical HONO flux above a northern Michigan forest canopy, Atmos. Chem. Phys., 12(17), 8285–8296, doi:10.5194/acp-12-8285-2012, 2012.

Zhang, N., Zhou, X., Shepson, P. B., Gao, H., Alaghmand, M. and Stirm, B.: Aircraft measurement of HONO vertical profiles over a forested region, Geophys. Res. Lett., 36(15), 1–5, doi:10.1029/2009GL038999, 2009.

Zhou, X., Beine, H. J., Honrath, R. E., Fuentes, J. D., Simpson, W., Shepson, P. B. and Bottenheim, J. W.: Snowpack Photochemical Production of HONO: a Major Source of OH in the Arctic Boundary Layer, Geophys. Res. Lett., 28(21), 4087–4090, doi:10.1029/2001GL013531, 2001.

Atmos. Meas. Tech. Discuss., doi:10.5194/amt-2016-17, 2016
Manuscript under review for journal Atmos. Meas. Tech.
Published: 25 January 2016

Atmospheric Measurement Techniques
Discussions

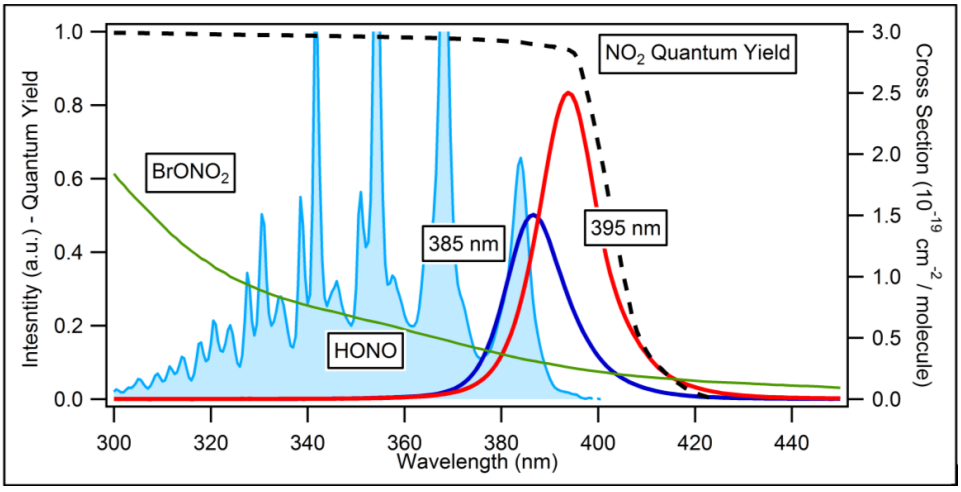

Figure 1. The measured spectral output of two UV-LED elements, nominally 385 nm output in dark blue, and 395 nm in red. The HONO absorption spectrum is shown in light blue whilst the NO_2 quantum yield is shown in dashed black. The absorption cross section of $BrONO_2$ is shown in green.

Atmos. Meas. Tech. Discuss., doi:10.5194/amt-2016-17, 2016
Manuscript under review for journal Atmos. Meas. Tech.
Published: 25 January 2016

Atmospheric Measurement Techniques Discussions

Table 1. Showing the distribution of NO_y species NO, NO_2, HNO_3, and HONO produced from the HONO permeation source.

#	NO_y ppb Measured	NO ppb Measured	NO_2 ppb Measured	HNO_3 ppb Calculated	HONO ppb Calculated
1	20.40	3.34	2.64	0.35	14.08
2	19.29	2.96	2.35	0.30	13.68
3	16.82	2.59	2.10	0.26	11.89
4	14.95	2.27	1.87	0.20	10.62
5	13.40	2.05	1.73	0.16	9.45
6	12.15	1.86	1.58	0.14	8.57
7	11.09	1.70	1.46	0.12	7.81
8	10.17	1.60	1.35	0.11	7.14
Percent	%	15.5	12.8	1.3	70.4

Atmos. Meas. Tech. Discuss., doi:10.5194/amt-2016-17, 2016
Manuscript under review for journal Atmos. Meas. Tech.
Published: 25 January 2016

Atmospheric Measurement Techniques Discussions

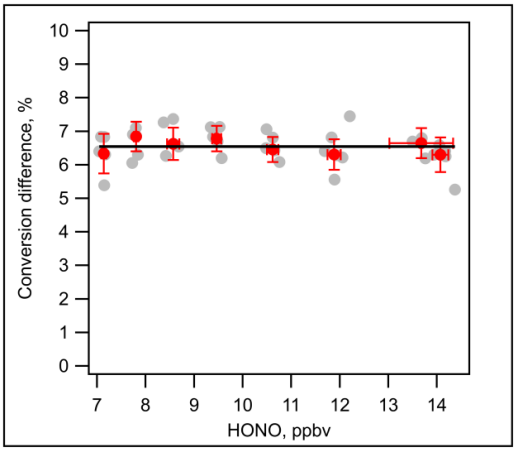

Figure 2. Difference in HONO conversion between 385 and 395 nm UV-LEDs over a range of dilutions. Median values are in red, while all data is shown in grey. Linear fit is in black.

Atmos. Meas. Tech. Discuss., doi:10.5194/amt-2016-17, 2016
Manuscript under review for journal Atmos. Meas. Tech.
Published: 25 January 2016

Atmospheric Measurement Techniques Discussions

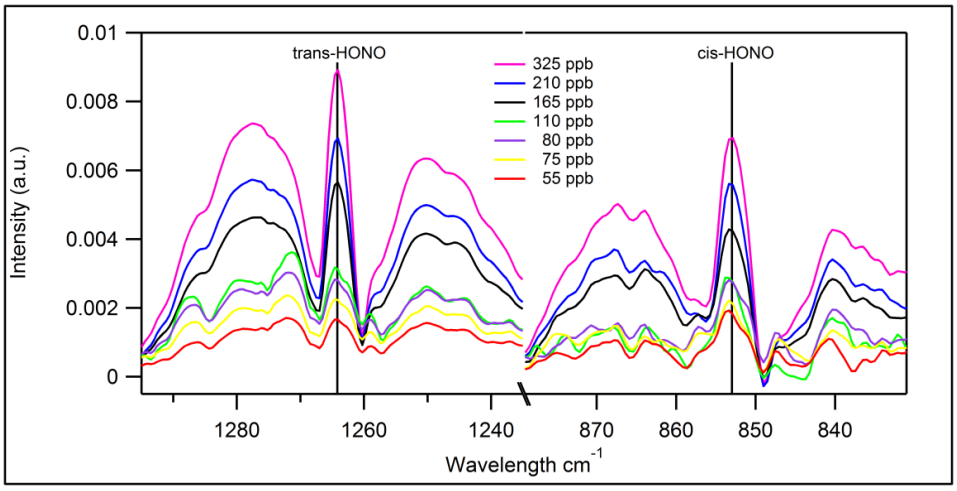

Figure 3. FT-IR spectra of dominant HONO absorbance lines at 1264, 853cm^{-1}, over a range of concentrations.

Atmos. Meas. Tech. Discuss., doi:10.5194/amt-2016-17, 2016
Manuscript under review for journal Atmos. Meas. Tech.
Published: 25 January 2016

Atmospheric Measurement Techniques Discussions

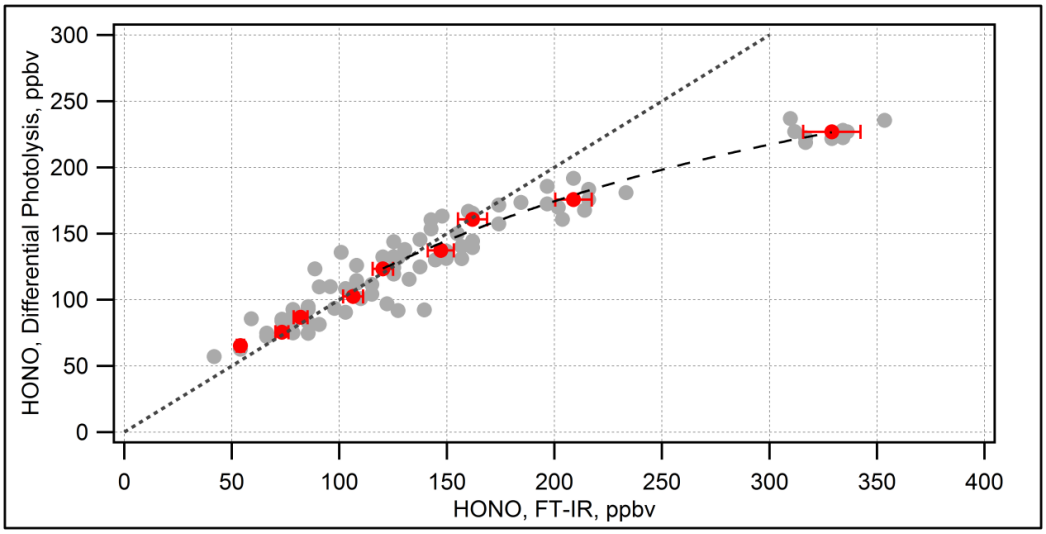

Figure 4. HONO determined by FT-IR (y-axis), versus HONO measured by the photolytic/chemiluminescence differential photolysis instrument (x-axis). Median values at each dilution are in red; all values are shown in grey. The 1:1 line is shown for reference as well as an exponential fit above 150 ppbV HONO.

Atmos. Meas. Tech. Discuss., doi:10.5194/amt-2016-17, 2016
Manuscript under review for journal Atmos. Meas. Tech.
Published: 25 January 2016

Atmospheric Measurement Techniques Discussions

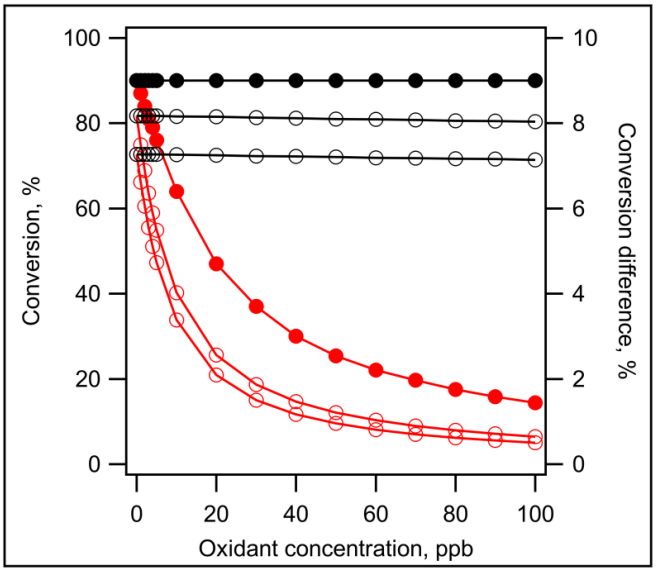

Figure 5. Simulated conversion (open circles), and different in conversion (closed circles) for photolytic converters with different j in the presence of OH (red) and O_3 (black) oxidants.

Atmos. Meas. Tech. Discuss., doi:10.5194/amt-2016-17, 2016
Manuscript under review for journal Atmos. Meas. Tech.
Published: 25 January 2016

Atmospheric Measurement Techniques Discussions

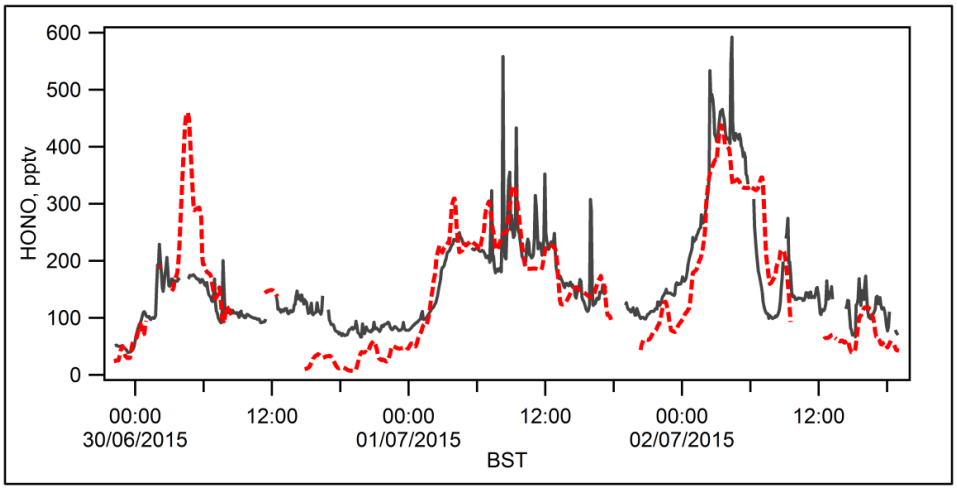

Figure 6. HONO time series during July 2015 at the Weybourne Atmospheric Observatory (WAO) measured by LOPAP (grey) and pHONO (red).

Atmos. Meas. Tech. Discuss., doi:10.5194/amt-2016-17, 2016
Manuscript under review for journal Atmos. Meas. Tech.
Published: 25 January 2016

Atmospheric Measurement Techniques Discussions

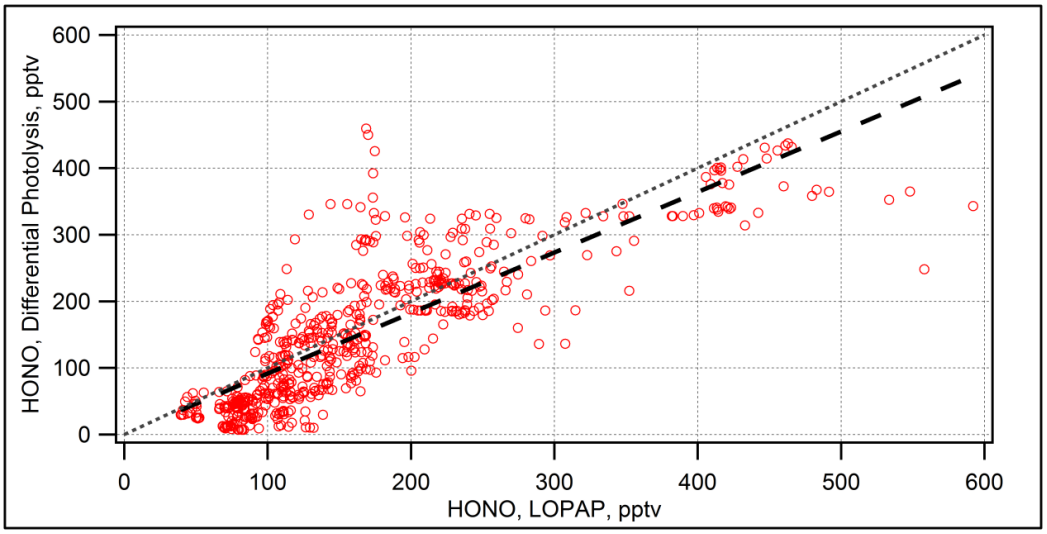

Figure 7. Correlation between HONO measured by LOPAP (x-axis) and pHONO (y-axis). The linear correlation is shown in black and the 1:1 line is shown for reference.